Journal of Thermal Analysis, Vol. 50 (1997) 547-558

MELTING OF INDIUM BY TEMPERATURE-MODULATED DIFFERENTIAL SCANNING CALORIMETRY

K. Ishikiriyama[*], *A. Boller and B. Wunderlich*[**]

Department of Chemistry, The University of Tennessee, Knoxville, TN 37996-1600, and Chemical and Analytical Sciences Division, Oak Ridge National Laboratory, Oak Ridge TN 37831-6197, USA

(Received December 4, 1996)

Abstract

The melting and crystallization of a sharply melting standard has been explored for the calibration of temperature-modulated differential scanning calorimetry, TMDSC. Modulated temperature and heat flow have been followed during melting and crystallization of indium. It is observed that indium does not supercool as long as crystal nuclei remain in the sample when analyzing quasi-isothermally with a small modulation amplitude. For standard differential scanning calorimetry, DSC, the melting and crystallization temperatures of indium are sufficiently different not to permit its use for calibration on cooling, unless special analysis modes are applied. For TMDSC with an underlying heating rate of 0.2 K min^{-1} and a modulation amplitude of 0.5–1.5 K at periods of 30–90 s, the extrapolated onsets of melting and freezing were within 0.1 K of the known melting temperature of indium. Further work is needed to separate the effects originating from loss of steady state between sample and sensor on the one hand and from supercooling on the other.

Keywords: indium, melting, temperature calibration, TMDSC

Introduction

Calibration of differential scanning calorimetry (DSC) is central for quality data. A special problem is the temperature calibration on cooling with sharply melting calibrants, because of the common supercooling before crystallization. On the development of temperature-modulated DSC (TMDSC) [1], it became paramount to find melting and crystallization standards that can serve as calibration materials and as a test substance for TMDSC in the presence of a first-order

* On leave from Toray Research Center, Inc., Otsu, Shiga 520, Japan.
**Author to whom all correspondence should be addressed.

0368–4466/97/ $ 5.00

John Wiley & Sons Limited
Chichester

transition. It will be shown in this paper that small amounts of indium can be used as such calibration standard for TMDSC for heating and cooling. As long as crystallization nuclei remain after the heating cycle, supercooling of the sharply melting indium is negligible. In this case one needs only to make corrections for the instantaneous heating rate of the sample just before melting or crystallization begins, making sure, as always, that steady state exists before the transition begins and the temperature gradient within the sample is small.

In a previous paper we explored the limits of TMDSC and developed the method of quasi-isothermal analysis [2]. Also, the question of linearity of TMDSC and attainment of steady state have been discussed [3] and a summary of the practice of TMDSC has been prepared [4]. More recently, it was shown that the problems that arise from remaining asymmetry can be resolved by either introducing a known imbalance, or by finding the phase difference between sample and base-line runs [5, 6].

It is well known that the melting temperature of calibrants such as indium depend on scanning rate [7], and hence there might be difficulties for the temperature calibration for TMDSC, because its scanning rate changes during its modulation cycle between 0 and $\pm 120\pi A/p$ K min^{-1}, where A is the maximum modulation amplitude in K of the sample temperature, T_s, and p is the modulation period in s. Since there are two techniques for measurements with TMDSC, namely the quasi-isothermal method and the continuous heating or cooling method with an underlying rate of temperature change $<q>$, calibration for both techniques will be explored.

In this paper, the transition temperatures of indium are examined. First as a function of scanning rate in standard DSC. This is followed by an analysis of the melting and crystallization temperatures with the two methods of TMDSC. Finally, a recipe is given for temperature calibration of TMDSC that involves linking the modulated temperature to the modulated heat flow in the transition region.

To modulate a DSC, one adds a sinusoidal oscillation to the block temperature T_b that would have increased linearly for standard DSC:

$$T_b = T_o + <q>t + A_{T_b}\sin(\omega t) \tag{1}$$

where T_o is the temperature at the beginning of the experiment; $<q>$, the underlying scanning rate; t, time; A_{T_b}, the amplitude of the modulation for the block temperature; and ω, the chosen modulation period in units of radians. Similarly, the steady-state sample temperature is:

$$T_s = T_o + <q>t - \frac{<q>\, C_s}{K} + A\sin(\omega t - \varepsilon) \tag{2}$$

where A is the maximum modulation amplitude of the sample temperature, set as a run parameter, and ε is the phase lag between the block temperature and the

sample temperature. During melting and crystallization of indium the sample temperature cannot change sinusoidally due to the exchange of latent heat, and the differences between sensor, program, and sample temperatures need to be evaluated. For this purpose an optimizing function has been derived that permits to identify the deviation of the sensor temperature from the sinusoidal modulation:

$$S_{opt} = \Sigma(T_s - T_o' - <q>t - A\sin(\omega t - \varepsilon))^2 \quad (3)$$

where $T_o' = (T_o - <q>C_s/K)$, $<q>$, A, and ε are determined at the minimum of S_{opt}. The deviation of the sensor temperature from the expected sinusoidal temperature lets one, then, find the sensor temperature at the beginning of melting and crystallization.

Experimental

An indium sample of 1.085 mg was measured with a commercial TMDSC of the Thermal Analyst 2910 system from TA Instruments Inc. (MDSC^{TM}). Dry nitrogen gas with a flow rate of 20 mL min^{-1} was purged through the DSC cell. The temperature of the MDSC equipment was initially calibrated in the standard DSC mode by using the transition peaks for cyclohexane (186.09 K), octane (216.15 K), water (273.15 K), and indium (429.75 K) at a scanning rate of 10 K min^{-1}. As usual, the melting point of sharply melting standards is chosen at the onset of melting. It is determined by extrapolating the sample temperature from the linear portion of the melting peak to the baseline [8]. Similarly, the onset of crystallization was extrapolated from the crystallization peak on cooling. The heat capacity of the small amount of indium is sufficiently small, so that the heat-capacity baseline of crystalline and liquid indium can be used for the intercept without calibration of its amplitude with the heat capacity of sapphire. This baseline is practically horizontal because of the only minor change of heat capacity of indium on melting. For heat of fusion measurement, the heat flow was calibrated with the heat of fusion of indium itself. Subsequently, the melting and crystallization transition temperatures of indium were measured as a function of scanning rate from ±0.2 to ±20.0 K min^{-1}, using both, the liquid-nitrogen cooling-accessory (LNCA) and the air cooling accessory. Quasi-isothermal measurements of the melting of indium were made with a low modulation amplitude of A=0.05 K, coupled with a period of p=60 s and stepwise temperature-increments of 0.1 K. Both the modulated temperature and heat flow were measured for ten minutes at each temperature. Finally, TMDSC runs with an underlying heating rate $<q>$=0.2 K min^{-1} were carried out. These standard TMDSC measurements of the melting of indium were conducted for the nine combinations of periods of 30, 60, and 90 s, and maximum amplitudes A of 0.5, 1.0, and 1.5 K. By analyzing the three combinations in the sequence of pairs as written, the instan-

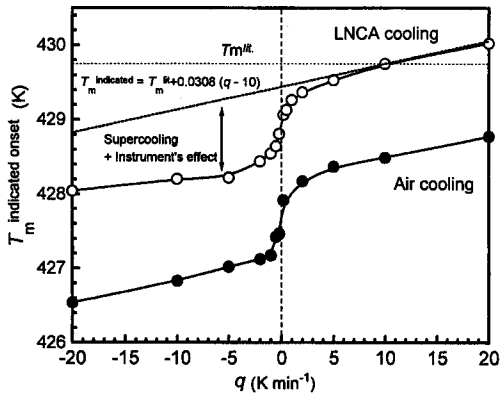

Fig. 1 The onset temperatures of melting and crystallization for indium as a function of temperature. Open and closed circles represent the data obtained with the liquid nitrogen cooling and air cooling accessory, respectively

taneous heating rate $q=\mathrm{d}T/\mathrm{d}t$ is the same at equal phase angles for all three periods, with maxima of the instantaneous heating rates of $q=6.5$ K min^{-1} and minima of $q=-6.1$ K min^{-1}. From Eq. (2) the heating rate can be seen to be equal to $<q>+A\omega\cos(\omega t-\varepsilon)$.

Results

Figure 1 shows the onset temperatures of melting and crystallization for indium as a function of scanning rate for the two cooling accessories (liquid-nitrogen cooling accessory, LNCA, and air cooling). In both configurations the onset of melting increases with scanning rate. The two almost linear branches are offset by about 1.0 K due to the crystal nucleation on cooling, as shown by the double arrow. The apparent transition temperatures measured with the liquid nitrogen cooling accessory are about 1.5 K higher than those measured with the air cooling accessory. After fitting the calorimeter to a heating rate of 10 K min^{-1}, the tangent to the indicated temperature is, as shown in Fig. 1:

$$T_{\mathrm{m}}^{\mathrm{indicated}} = T_{\mathrm{m}}^{\mathrm{literature}} + 0.0308(q - 10) \tag{4}$$

Note, that the fitting is done to the heating branch. There seems to be, depending on the cooling mode, a small asymmetry in the cooling and heating branches of the curves of Fig. 1. Also, the sigmoidal shape in going through zero heating rate is in need of further discussion.

The melting of indium measured under quasi-isothermal conditions is shown in Fig. 2. Below and above 429.345 K the heat flow is small and sinusoidal, as expected from the low heat capacity of the sample. When the temperature is modulated at 429.345±0.05 K, the amplitude of the heat flow increases substan-

tially due to the much larger melting and crystallization effect. Note that the chosen maximum amplitude A in Eq. (2) is governed in the MDSC of TA Instruments by changing the maximum amplitude A_{T_s} to such a degree that the proper modulation A is reached at the sample temperature sensor, a condition nearly achieved in the experiment of Fig. 2. Naturally, during melting the sample temperature stays largely constant at T_m, in contrast to the sensor temperature.

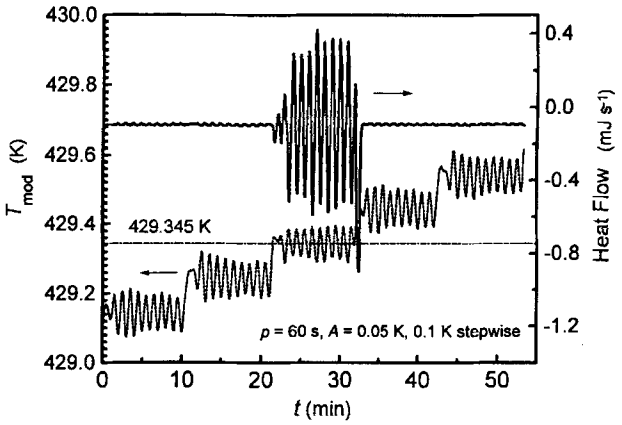

Fig. 2 Melting of indium measured under quasi-isothermal conditions

A section of a typical result of the melting of indium measured with an underlying heating rate <q> of 0.2 K min^{-1} is shown in Fig. 3. The solid curve represents the heat flow. It increases also strongly in the endothermic melting and exothermic crystallization regions of the indium. The dash-dotted curve of the sample-temperature sensor remains close to sinusoidal, but has deviations in the

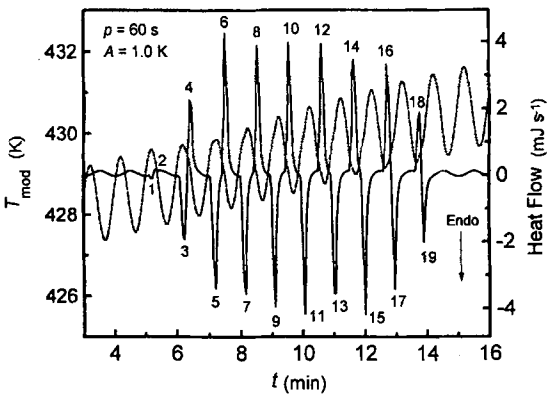

Fig. 3 The modulated heat flow and sample sensor-temperature for melting and crystallization of indium on continuous heating with an underlying heating rate of 0.2 K min^{-1}

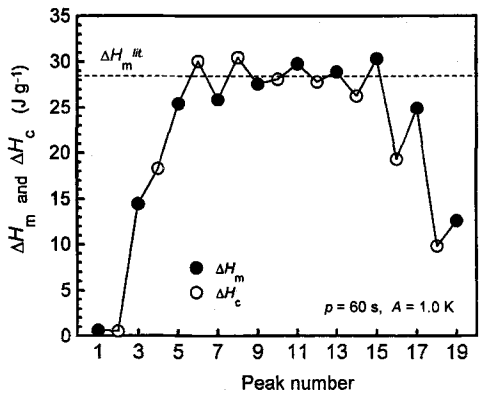

Fig. 4 The peak areas, i.e., the enthalpy change on melting and crystallization of indium calculated by integration of the endothermic and exothermic peaks of Fig. 3

melting and crystallization regions. The endothermic melting peaks are marked by increasing odd numbers, the exothermic crystallization peaks, by even numbers.

The peak areas in Fig. 3 for melting and crystallization, ΔH_m and ΔH_c, taken over an approximate baseline, are summarized in Fig. 4. Peaks 5 to 15 agree with the transition enthalpy of indium, known to be 28.45 J g^{-1} [9]. The change of the average temperature of the sensor during the multiple meltings is about (9 min×0.2 K min^{-1})=1.8 K, the crystallizations, 1.6 K.

Discussion

The onset temperatures measured by standard DSC of melting and crystallization depend on the scanning rate and the type of cooling accessory used, as shown in Fig. 1. Both, the scanning-rate and accessory dependence is due to the temperature difference between sample and sensor (the sample thermocouple). The initial calibration was done at 10 K min^{-1} as indicated in the figure. The limiting slopes of the heating and cooling experiments are somewhat different and the difference seems also to depend on the cooling mode. This scanning-rate dependence of the indicated (sensor) temperatures on melting and crystallization of indium in standard DSC suggests that the indicated (sensor) temperature during TMDSC must be even more complicated because of the continuous change in scanning rate on modulation.

The gap of about one kelvin between the heavy dashed line in Fig. 1, expressed by Eq. (4), and the equivalent data measured on cooling is obviously due to the need of nucleation of crystal growth (supercooling). The sigmoidal rounding of this jump, leading seemingly to smaller supercoolings at low cooling rates and lower melting temperatures on slow heating has its origin in the inability of

the sample to follow the linear temperature increase during the phase transition, i.e. after the onset temperatures. Steady state requires that heater, sample, and sensor temperatures change with the same rate [8]. As melting begins at the bottom of the sample, its temperature is fixed at T_m. The heating rate is governed, however, by the sensor temperature, i.e. it is forced up by additional heat input regardless of the sample temperature. As a result, the temperature differences from sample to heater and sample to sensor increase. This sets up an additional heat flow between sensor and sample, resulting in the deviation from the expected temperature of Eq. (4). On melting, the sample temperature decreases relative to the sensor temperature, on crystallization, it increases, distorting the crystallization peak with an additional heat flow out of or into the sensor, respectively. For the faster rates of temperature change this effect becomes negligible. Obviously this rounding of the temperature lag about zero rate of temperature change is dependent on the sample mass, placement and geometry of the pan, as well as the overall DSC construction and running conditions. In the present case the effect seems to be able to cause an effect of close to 0.5 K.

Preliminary experiments with liquid crystal transitions in our laboratory which are known to show no supercooling also showed deviations of similar magnitudes at low rates of temperature change. A quantitative analysis was, however, not possible because of insufficient symmetry of the inherently broad transitions of liquid crystals and the much lower heat of transition than for indium. To date, liquid crystals seem to have been studied in more detail only with power-compensation DSC for calibration as a function of heating rate [10, 11]. In these instruments, the heat-flux problems on melting needs a different discussion [8].

The quasi-isothermal experiments of Fig. 2 reveals the remarkable increase in modulation amplitude of the heater (temperature, T_b) which is needed to accomplish the increased heat flow in the melting and crystallization range. Based on the fact that only one quasi-isothermal step shows any melting and crystallization, one can establish the run at 429.345±0.05 K as occurring at the sensor temperature of melting. The literature value of the melting temperature of indium is 429.75 K [7], 0.4 K higher than T_o. The difference between the measured and expected value is close to the calibration of the calorimeter to a heating rate of 10 K min^{-1} (0.3 K). There is no indication of the supercooling of one kelvin expected from the standard DSC results of Fig. 1. The reason for this missing supercooling will be shown next to be the incomplete melting in the quasi-isothermal cycles at 429.345 K. On going to 429.445 K melting is complete, but crystallization is not possible anymore because nucleation is possible only at about 428.7 K.

To investigate the melting and crystallization further, the center portion of Fig. 2 is expanded in Fig. 5 with each peak labeled with its enthalpy of transition. In the center region, the heats of transition are about 5–8 J g^{-1}. This is much less than the known heat of fusion of 28.45 J g^{-1}. The time available during the heat-

ing cycle was, thus, too short to completely melt the sample. Adding all endotherms and exotherms in Fig. 5, yields 31.9 J g^{-1} which is within the error limit the total heat of fusion of the original crystals. More than 2/3 of the final fusion (20.4 J g^{-1}) occurred during the heating to the next higher temperature segment of the experiment (Fig. 5). Beyond this final melting peak the normal, shallow heat flow oscillations due to heat capacity are resumed.

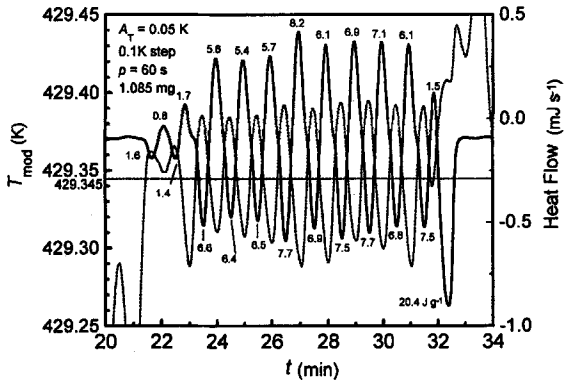

Fig. 5 Enlargement of the central part of Fig. 2 with indicated peak areas in J g^{-1}

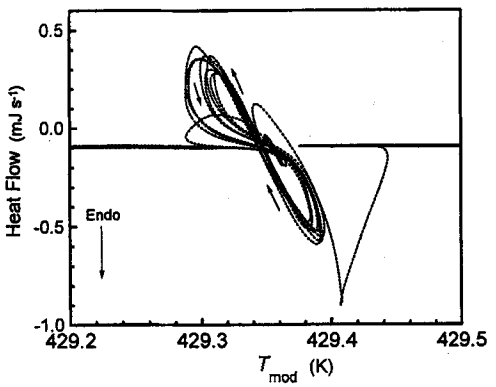

Fig. 6 Lissajous figure of the data in Figs 2 and 5

The melting/crystallization can be assessed in more detail from the Lissajous trace of heat flow *vs.* temperature in Fig. 6. On the left and right of the central figure are the steady-state ellipses, caused by the heat capacities of the solid and liquid at lower and higher temperatures, respectively. Their heat flows are small, so that the small axes of the ellipses deviate only little from the horizontal line. The melting and crystallization produces the slanted figure eight with the large deviation to the right representing the jump to the next higher T_0 (429.445 K). The

switch from melting to crystallization is continuous without visible break for supercooling in the sensor temperature. The melting loop is more repeatable than the crystallization loop. After the second crystallization peak in Fig. 5 of 1.7 J g^{-1}, the heat flow starts to repeat itself. Similarly, the Lissajous figures show a break after each crystallization, reaching almost steady state before renewed melting. It occurs about 0.01 K above the base temperature of modulation.

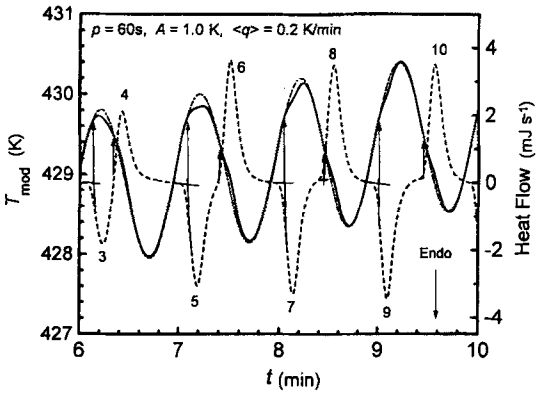

Fig. 7 Enlargement of Fig. 3 for the peaks 3–10. The broken curve represents the heat flow. The solid and dash-dotted curves represent the observed and expected sinusoidal sample temperatures, respectively, making use of the optimization of Eq. (3)

The normal TMDSC trace of Fig. 3 is evaluated next. A magnified portion is shown in Fig. 7 and the corresponding Lissajous figures are displayed in Fig. 8. Note that the heat flows at the melting and crystallization peaks are almost 10× bigger than in the quasi-isothermal experiments. The dash-dotted curve in Fig. 7 is the sinusoidal temperature program, reconstructed from the optimization function given as Eq. (3). The onset times extrapolated from the endothermic and exothermic peaks of the dashed heat-flow curves are marked by the vertical arrows ending at the corresponding temperatures and summarized in Fig. 9. The arrows point to the onsets of deviation in the temperature modulation due to melting and crystallization. The initial melting/crystallization peaks 1, 2 and 3, 4 of Fig. 3 show incomplete melting and are similar to the quasi-isothermal data of Figs 5 and 6. The same is true for the final crystallization and melting peaks 16, 17 and 18, 19. Between these two limits, considerable progress towards steady state is made on the left after crystallization and before melting (see 4, 5 and 6, 7 in Fig. 7), and then on the right after melting and before crystallization (see 13, 14 and 15, 16 in Fig. 3). The Lissajous figures (Fig. 8) summarize all approaches to equilibrium. The missing one kelvin supercooling can be taken as an indication that in all cases enough self-nuclei remain to restart crystallization as soon as the temperature drops below the melting point.

A tabulation of the 47 onset temperatures of melting at modulation periods of 60 and 90 s give an average and RMS-deviations of 429.8±0.2 K. This is close to

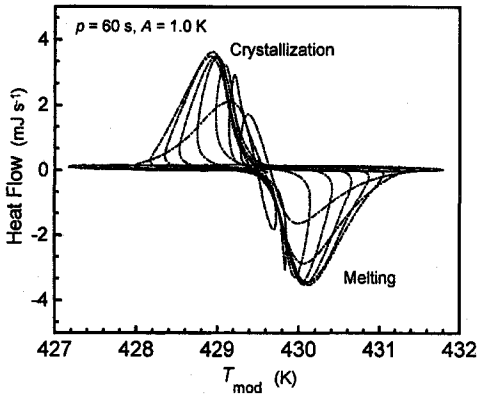

Fig. 8 Lissajous figure of the data in Figs 3 and 7

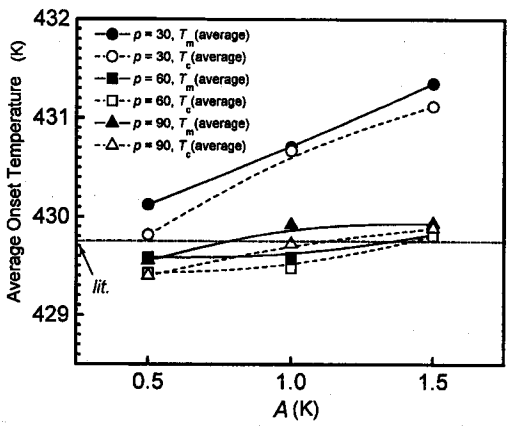

Fig. 9 The averages of the indicated onset temperatures for melting and crystallization of indium as a function of maximum amplitude for different modulation periods

the onset of the melting temperature for standard DSC at 10 K min^{-1}, shown in Fig. 1 (429.75 K). The experiments with modulation periods of 60 and 90 s have maximum heating rates in the range 2.3 to 9.6 K min^{-1}, i. e. the averages of the tabulation are almost within the error limit of Eq. (4). Any effort to improve the onset temperatures by correcting for the instantaneous cooling rates using Eq. (4) or even the actual data of Fig. 1, was unsuccessful. A more detailed study of the temperature lags that change the slopes of the melting peaks is needed to increase the precision. The rounding of the curves of the indicated onset temperatures in Fig. 1 in the vicinity of zero heating an cooling rates was a similar indication of major deviations from steady state in the melting range. New experiments with lower sample masses and control of the reference calorimeter instead of the sample calorimeter are being undertaken to resolve these problems and increase precision of calibration [12].

A tabulation of the 41 onset temperatures of crystallization at modulation periods of 60 and 90 s gives an average and RMS-deviations of 429.7±0.2 K, 0.1 K less than the extrapolated melting temperatures. A similar difference of 0.2 K can be seen in Fig. 8. Although this is the order of magnitude of the temperature correction expected on changing from heating to cooling (0.1 to 0.6 K), it is not safe to make this conclusion, particularly since individual correction of the data gives no better fit.

In Fig. 9 all averages of the data sets are plotted according to their run parameters. The melting and crystallization data for the modulation period of 30 s change more rapidly with modulation amplitude than expected from Fig. 1 (maximum heating rates 6.5, 12.8, 20 K min^{-1}, observed increase in T_m, 1.2 K rather than 0.4), those of the 60 and 90 s runs with maximum heating rates ranging from 2.3, to 9.6 K min^{-1} increase by 0.3 K, closer to the expected change.

The best recipe to calibrate TMDSC is at present the use indium at small modulation amplitudes and quasi-isothermal conditions as shown in Fig. 2. By using sufficiently closely spaced temperature steps, the melting temperature can be established for close-to-zero heating rates. For use of an underlying heating rate the precision is less, but Fig. 9 shows that for periods of 60 to 90 s and amplitudes of 0.5 to 1.5 K the calibration data of standard DSC at 10 K min^{-1} are usable with an empirical accuracy of ±0.2 K. There exist large deviations between indicated and actual sample temperature, and the steady state is interrupted. Similar evaluation techniques as were developed for standard DSC in the melting range in form of the "baseline-method" [8] must be developed for TMDSC. Efforts in this direction will be reported later [12].

* * *

This work was supported by the Division of Materials Research, National Science Foundation, Polymers Program, Grant # DMR 90-00520 and the Division of Materials Sciences, Office of Basic Energy Sciences, U.S. Department of Energy at Oak Ridge National Laboratory, managed by Lockheed Martin Energy Research Corp. for the U.S. Department of Energy, under contract number DE-ACOS-960R22464. Support for instrumentation came from TA Instruments, Inc. and Mettler-Toledo Inc. Research support was also given by ICI Paints.

References

1 M. Reading, Trends in Polymer Sci., 8 (1993) 248; P. S. Gill, S. R. Sauerbrunn, and M. Reading, J. Thermal Anal., 40 (1993) 931; M. Reading, D. Elliot, and V. L. Hill, J. Thermal Anal., 40 (1993) 949.
2 A. Boller, Y. Jin and B. Wunderlich, J. Thermal Anal., 42 (1994) 307–330.
3 B. Wunderlich, A. Boller, I. Okazaki and S. Kreitmeier, Thermochim. Acta, 282/283 (1996) 143.
4 B. Wunderlich, "Modulated Differential Thermal Analysis." A computer assisted lecture course of 99 screens, published on World Wide Web (URL: http://funnelweb. utcc. utk. edu.~athas) 1995.
5 K. Ishikiriyama and B. Wunderlich, J. Thermal Anal., 50 (1997) 337.

6 A. Boller, I. Okazaki, K. Ishikiriyama, G. Zhang and B. Wunderlich, J. Thermal Anal., 49 (1997) 1081.
7 H. K. Cammenga, W. E. Eysel, E. Gmelin, W. Hemminger, G. W. H. Höhne and S. M. Sarge, Thermochim. Acta, 219 (1993) 333.
8 B. Wunderlich, "Thermal Analysis," Academic Press, Boston, 1990.
9 S. M. Sarge, E. Gmelin, W. H. Höhne, H. K. Cammenga, W. Hemminger and W. Eysel, Thermochim. Acta, 246 (1994) 319.
10 J. D. Menczel and T. M. Leslie, Thermochim. Acta, 166 (1990) 309.
11 G. W. H. Höhne, J. Schawe, and C. Schick, Thermochim. Acta, 221 (1993) 129.
12 A. Boller, M. Ribeiro, and B. Wunderlich, to be completed.